Supplemental Data

Conduits Mediate Transport of Low-Molecular-Weight Antigen to Lymph Node Follicles

Ramon Roozendaal, Thorsten R. Mempel, Lisa A. Pitcher, Santiago F. Gonzalez, Admar Verschoor, Reina E. Mebius, Ulrich H. von Andrian, and Michael C. Carroll

Supplemental Experimental Procedures

Multiphoton intravital microscopy (MP-IVM)

Mice were anaesthetized with ketamine (100 mg/kg bodyweight) and xylazine (10 mg/kg bodyweight) and positioned on a custom-built microscope stage for microsurgical preparation of the right pLN, preserving afferent lymph and blood supply. Various combinations of reagents in volumes not exceeding 10 µl were injected s.c. into the right footpad during or at indicated time-points before image acquisition. Multiphoton imaging was performed on an Ultima IV upright multiphoton microscope (Prairie Technologies, Middleton, WI) equipped with either an Olympus 20x/0.95 NA or an infrared-optimized Olympus 60x/1.1 NA water immersion objective, controlled by Prairieview software. For multiphoton excitation and second harmonic generation, two Ti:sapphire lasers with 10-W MilleniaXs pump lasers (Mai Tai HP and DeepSee, Spectra-Physics, Mountain View, CA) were tuned to wavelength between 800 nm and 1020 nm for balanced excitation of all fluorochromes used in a particular experiment. For four-dimensional recordings of cell motility and Ag transport, stacks of 2 to 11 optical sections were acquired every 5-15 seconds for 15 to 60 min with optical zoom up to 4X to provide image volumes of 2 to 40 µm in depth and 138 to 614 µm in width. Emitted light and second harmonic signals were detected through 460/50 or 525/50, 595/50 and 660/40 nm bandpass filters with non-descanned detectors to generate four-color images. For optimal visualization of EGFP and either A568 or A633, the same sample volume was recorded consecutively at 820 and 920 nm excitation wavelength and the resulting images overlaid. For simultaneous visualization of these fluorochrome combinations, the laser was tuned to 880 nm. Sequences of image stacks were transformed into volume-rendered, four-dimensional movies using the brightest-spot rendering mode within Volocity software (Improvision, Coventry, UK) and exported as Quicktime movies. Additional background subtraction was done using Photoshop (Adobe). Motion-artifacts in recordings were corrected using the auto-alignment plugin (stackreg) of ImageJ (http://rsb.info.nih.gov/ij/), which was also used to measure fluorescence intensities in non-volume rendered maximum intensity projections.

TEL trafficking

Unimmunized B6 mice were injected subcutaneously with 10 µg A488-TEL in the flank and base of tail to follow the draining of TEL in unimmunized mice. Inguinal lymph nodes were isolated at various time-points, fixed in 1% PFA followed by incubation in 30% sucrose and embedded in OCT for histological analyses.

Generation of Chimeric Mice

(B6) or CD45.1 mice were irradiated with two doses of 650 Rads four hours apart. Sixteen hours later, irradiated mice received 2 x 10^6 red blood cell-depleted bone marrow cells isolated from the femurs of B6 or CR2-deficient mice. Immune complex uptake by chimeric B cells was assessed at least eight weeks after generation of chimeras.

Figure S1

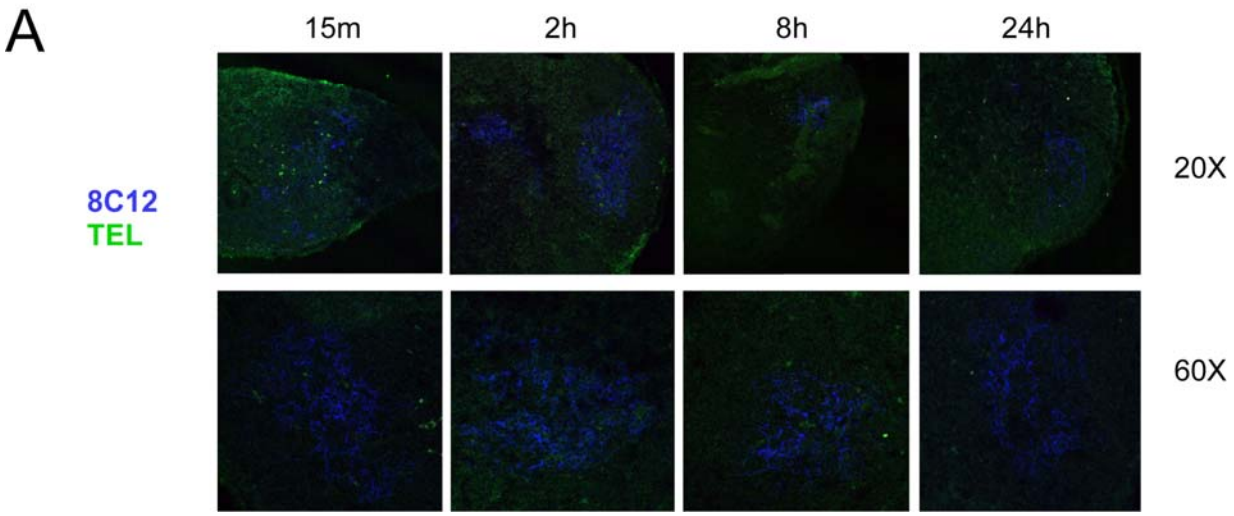

Figure S1. Trafficking of TEL in unimmunized mice. Unimmunized WT mice were injected subcutaneously in the hind flanks with 10 μg A488-TEL. The draining inguinal lymph nodes were harvested at 15 minutes, 2, 8 or 24 hrs post-injection, fixed in 1% PFA, 30% sucrose and embedded in OCT for histology using anti-CD35 antibodies to detect FDC.

Figure S2

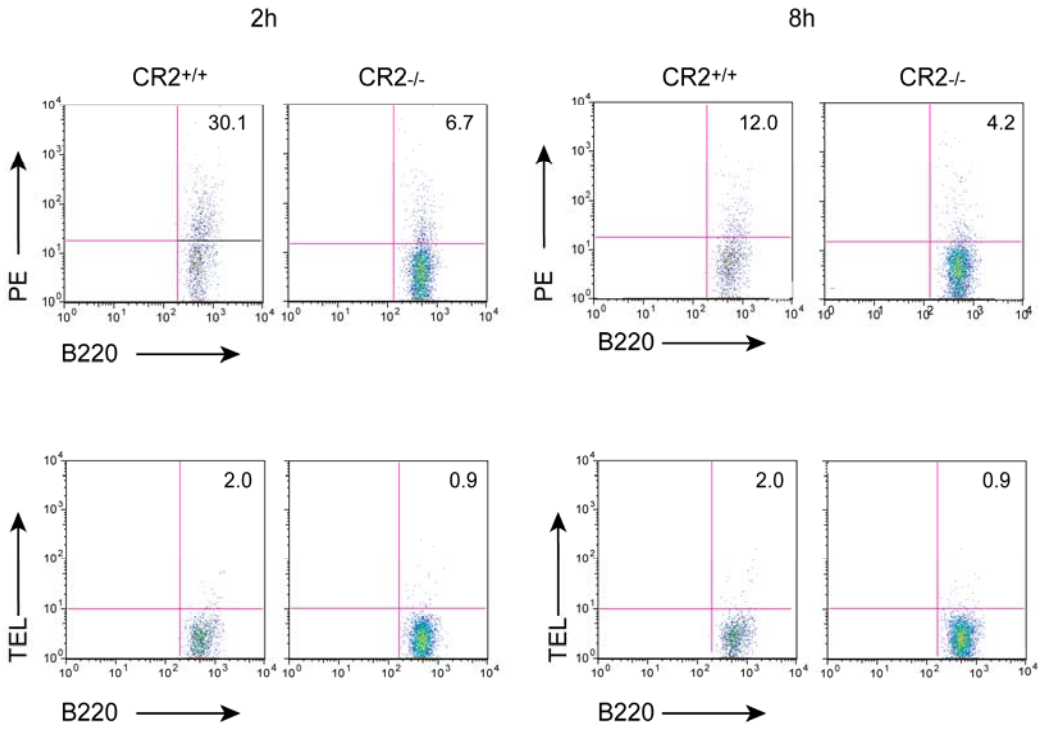

Figure S2. B cell transport of immune complexes is dependent on complement receptors CD21/35. Mixed bone marrow chimeric mice containing $Cr2^{+/+}$ and $Cr2^{-/-}$ B cells were passively immunized with antibodies against TEL and B-PE. Twenty-four hrs later, a mixture of 10 μg A488-TEL and 10 μg B-PE were injected subcutaneously into the flank and base of tail. At 2 and 8 hrs after injection, the inguinal lymph nodes were isolated, labelled with antibodies specific for CD21/35 and B220 and analyzed by flow cytometry.

Figure S3

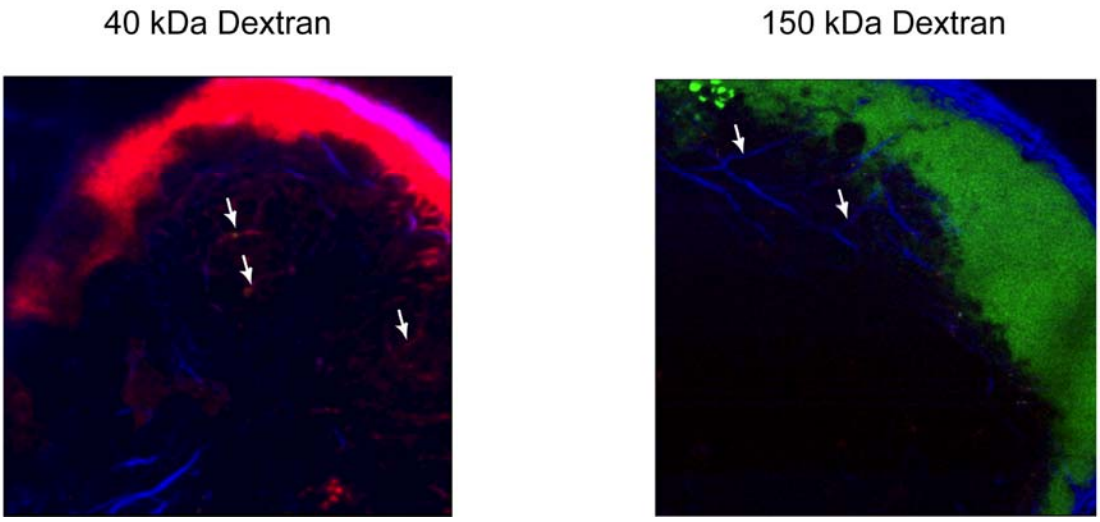

Figure S3. Antigen trafficking through the follicular conduits is size dependent. Fluorescently labelled Dextrans of 40 and 150 kDa were injected s.c. into the footpads of mice and their entry into the draining lymph nodes monitored by MP-IVM. White arrows indicate follicular conduits (detected by the second harmonic signal).

Figure S4

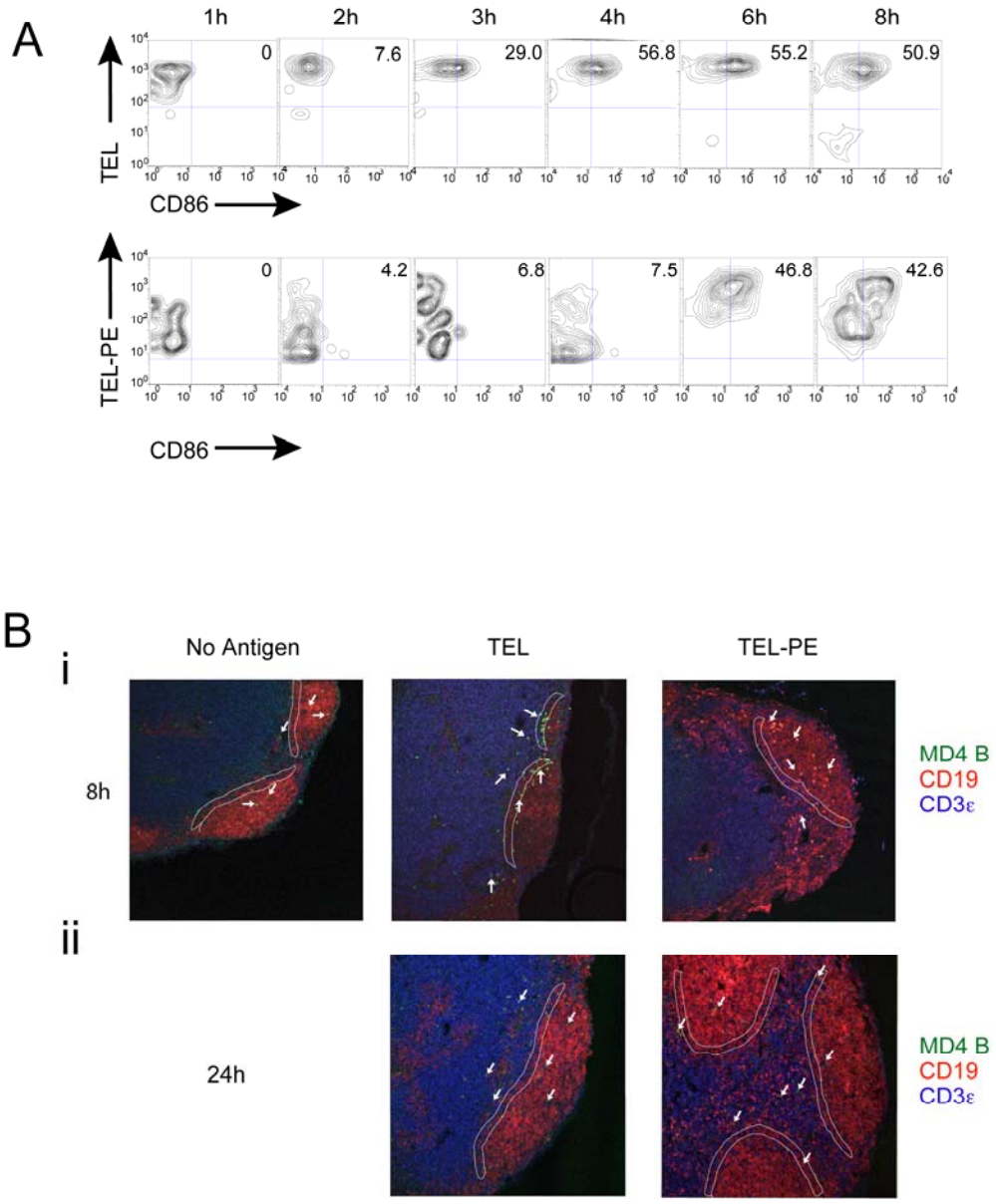

Figure S4. MD4 B cells are differentially activated by small versus large TEL antigens. A. Activation of MD4 B cells by TEL or TEL-PE was assessed by upregulation of CD86 cell surface expression by flow cytometry. Density plots, gated on adoptively transferred MD4 B cells were analyzed for CD86 expression at 1, 2, 3, 4, 6 and 8 hrs after antigen administration. B. Confocal microscopic analysis of MD4 B cell localization in the inguinal lymph nodes of mice was analyzed at 8 (i) or 24 (ii) hrs after antigen injection. Antibodies specific for CD45.2 (green), CD19 (red) and CD3ε (blue) were used to label MD4 B cells, B cells and T cells, respectively. The numbers of MD4

B cells localized in two distinct zones, within the follicles or within the T-B border or extrafollicular areas were determined by outlining the follicle and setting a T-B border zone, a ROI 22 μm into the follicle from the edge of the follicle distal the subcapsular sinus.

Figure S5

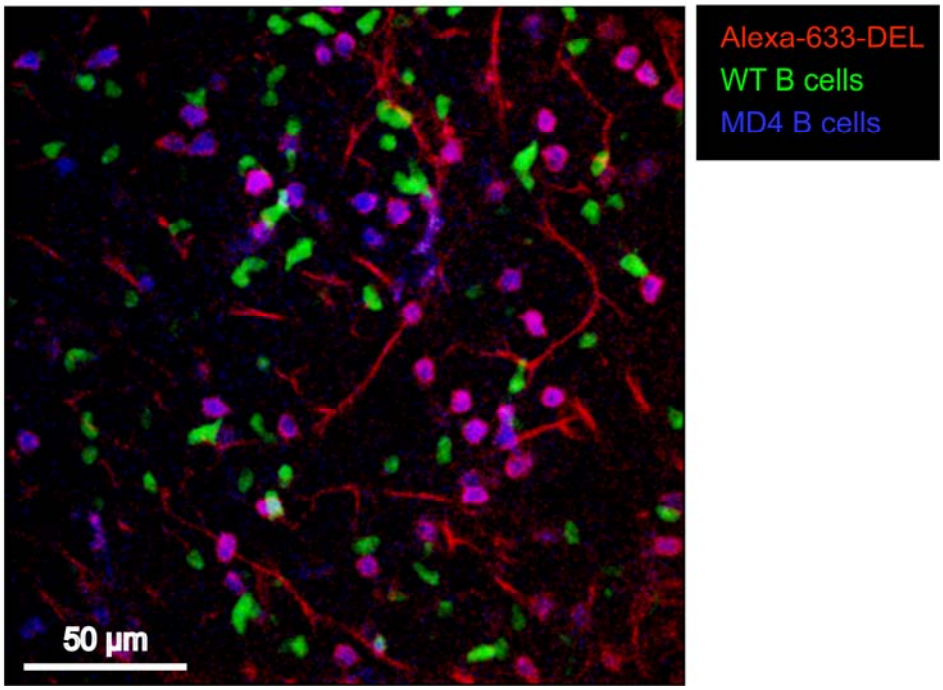

Figure S5. Low affinity antigen duck egg lysozyme (DEL) rapidly accumulates on MD4 B cells. 0.5 µg of Alexa Fluor 633-labeled DEL (red) was injected in 10 µl saline into the footpad of a mouse adoptively transferred 24 hours earlier with 20 x 10^6 each of purified polyclonal B cells (green) and MD4 B cells (blue). This micrograph was recorded 5.5 minutes after injection of DEL, when conduits were already filled and MD4 B cells coated with DEL.

Figure S6

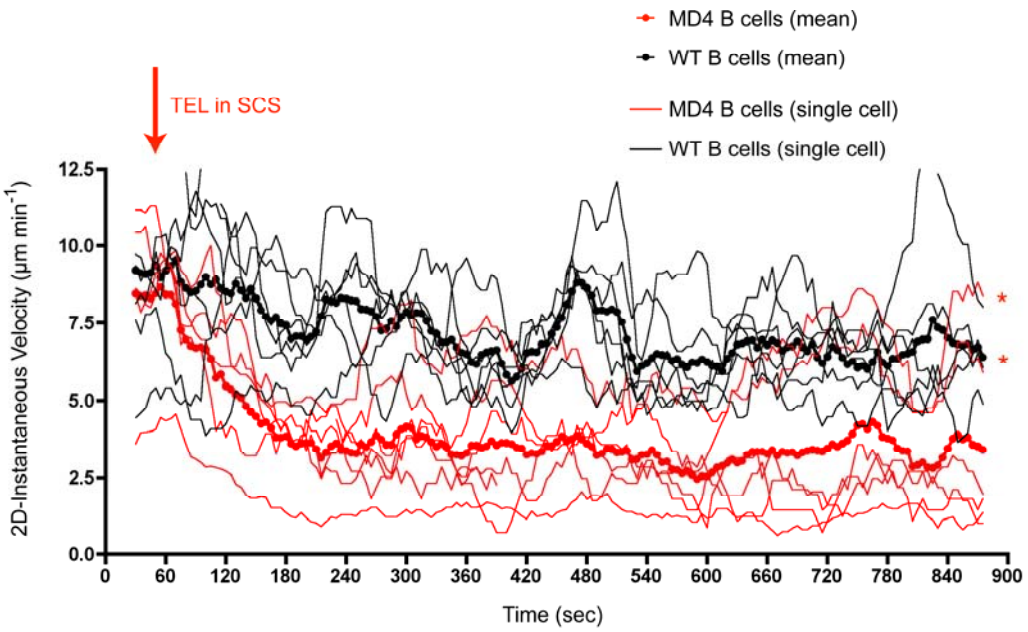

Figure S6: Binding of cognate antigen induces a transient deceleration of B cell motility. Migratory tracks of MD4 or control B cells in the popliteal lymph node (see supplementary movie 1) were selected based on their comparable velocities before the injection of antigen. Their time-averaged (±5 data points) instantaneous velocities were measured during and after footpad injection of fluorescently labeled TEL. Within seconds after arrival of TEL in the SCS (indicated by the red arrow), the motility of TEL-binding MD4, but not of control B cells, rapidly decreases. Two of the recorded velocity traces (marked by red asterisk), show recovery of baseline MD4 B cell migratory activity within the duration of the recording (15 min.).

Figure S7

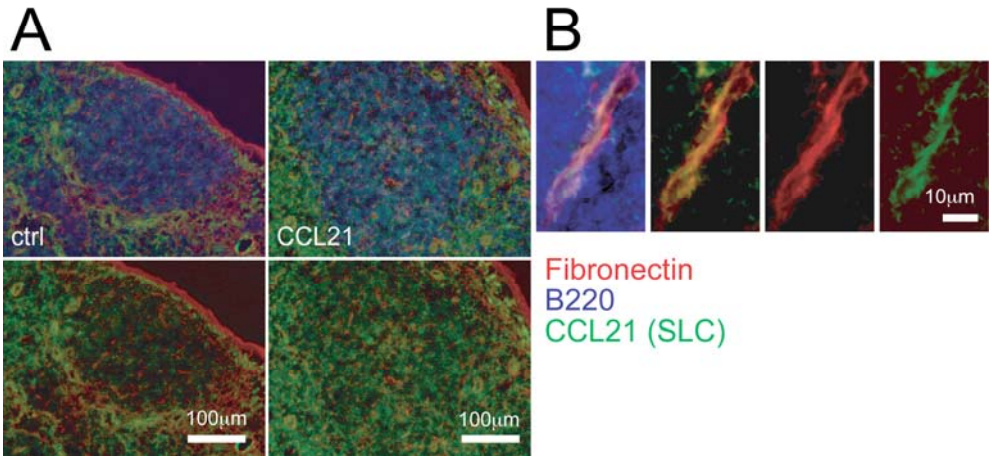

Figure S7. CCL21 rapidly distributes through LN follicles and associates with conduits. CCL21 (1 μg, SLC) was subcutaneously injected into the footpad. Draining lymph nodes were immediately fixed with 1% formaldehyde via the lymph for 15 minutes, and for 30 minutes in 1ml 1% formaldehyde afterwards. A. Fluorescence micrographs of popliteal lymph nodes from control (left panels) and CCL21 (anti-SLC-biotin, R&D Biosystems, Streptavidin-Alexa488, green) injected mice (right panels), showing that injected CCL21 rapidly distributes throughout the B-cell follicle as identified by B220 (blue) and fibronectin (red). Scale bar = 100 μm. B: Fluorescence micrograph of popliteal lymph node from a CCL21 (green) injected mouse, showing that injected CCL21 associates with conduits (fibronectin, red) in B-cell follicles (B220, blue). Scale bar = 10 μm. Images shown are representative of at least 2 independent experiments.